Journal of Electrotechnology, Electrical Engineering and Management (2024)
Clausius Scientific Press, Canada
DOI: 10.23977/jeeem.2024.070102
ISSN 2560-6697 Vol. 7 Num. 1

Performance Study of Lithium-Sulfur Batteries Based on Sulfur Cathode Thickness

Tingting Hu[1,a], Chunai Dai[1,b,*]

[1]*School of Physical Science and Engineering, Beijing Jiaotong University, Beijing, China*
[a]*21121671@bjtu.edu.cn*, [b]*chadai@bjtu.edu.cn*
[*]*Corresponding author*

Keywords: Electrochemistry, Lithium-Sulfur Battery, Sulfur Cathode

Abstract: With the deepening of energy structure transformation, new energy sources such as photovoltaics and wind power are important means to achieve carbon neutrality in the future. In order to solve the instability problem of their use, research on electrochemical energy storage systems has become a key aspect. In addition, lithium-ion batteries play an important role in electronic devices, but their lower theoretical specific capacity makes it difficult to meet the needs of large electronic devices. Lithium-sulfur batteries have a theoretical specific energy density (2600 Wh kg^{-1}) and theoretical specific capacity (1675 mAh g^{-1}) several times higher than lithium-ion batteries, and they have abundant elemental sulfur reserves and low prices. Therefore, lithium-sulfur batteries are very promising energy storage devices. The positive electrode material has an important impact on the performance of lithium-sulfur batteries and has been widely studied. This article investigates the effect of different sulfur cathode thicknesses on the performance of lithium-sulfur batteries.

1. Introduction

The traditional fossil energy reserves, represented by coal and oil, are increasingly depleted, and the extensive use of traditional fossil energy has also led to the gradual deterioration of the ecological environment [1]. Therefore, exploring green usage patterns of energy materials and developing new types of green energy are of great strategic significance for the sustainable development of human society. Although renewable energy sources such as solar energy, wind energy, geothermal energy, etc. can effectively meet human energy needs, the relative lag in energy storage technology cannot achieve their large-scale application. Therefore, developing high stability and long-life energy storage devices is considered the key to solving the problem of efficient energy utilization [2]. Lithium-sulfur batteries are considered the next generation energy storage system that is currently closest to practicality and has the most promising application prospects. Lithium-sulfur batteries not only have an ultra-high theoretical energy density, but also exhibit significant advantages in future energy system competition due to their wide range of elemental sulfur sources, low cost, high safety, environmental friendliness, and wide distribution [3]. Among the known cathode materials, elemental sulfur has a high theoretical specific capacity of 1 675 mAh g^{-1}, and the theoretical energy density of lithium-sulfur batteries composed of lithium metal anode is as high

as 2 600 Wh kg^{-1}, which is 3 ~ 5 times that of traditional lithium-ion batteries [4].

The reaction mechanism of Li-S battery is different from that of the ion mechanism in traditional lithium-ion batteries, and is closer to the electrochemical mechanism [5]. The reaction principle of lithium-sulfur battery is redox reaction, and the working principle of charge and discharge is shown in Figure 1. When a lithium sulfur battery begins to discharge, the lithium in the negative electrode reacts by losing electrons, generating Li+. Li+ migrates to the surface of the positive electrode through the electrolyte, while sulfur reacts with Li+ in the positive electrode by acquiring electrons, forming sulfides. The difference in potential between the positive and negative electrodes is the discharge voltage of the lithium sulfur battery. During charging, the reaction process of the electrode is opposite to that during discharge. When a voltage is applied, the chemical reaction between the positive and negative electrodes in a lithium sulfur battery proceeds in reverse, which is its charging process. The potential difference during the positive and negative electrode reaction process is the discharge/charging voltage of the lithium-sulfur battery.

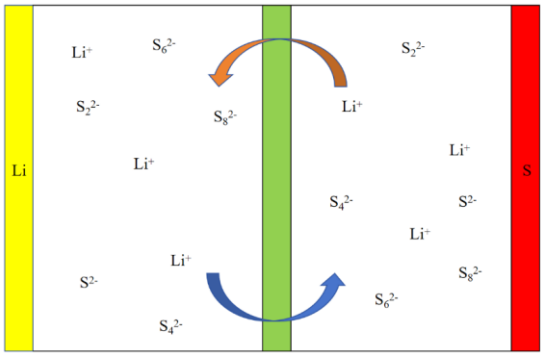

Figure 1: He charging and discharging working principle of L-S battery.

The reaction process of charging and discharging of lithium-sulfur battery is shown in equation:
Total battery reaction is shown as:

$$S_8 + 16Li \Leftrightarrow 8Li_2S. \quad (1)$$

Reaction of the sulfur positive electrode is shown as:

$$S_8 + 16Li^+ + 16e \Leftrightarrow 8Li_2S. \quad (2)$$

Reaction of lithium metal anode is shown as:

$$16Li \Leftrightarrow 16Li^+ + 16e. \quad (3)$$

Although the research on lithium-sulfur battery started as early as 50 or 60 years ago, there are still some urgent problems that hinder the commercial application of lithium-sulfur battery. Among these series of problems, weak conductivity and cycle instability are the key problems hindering its commercial production. Efforts have been made to solve this problem, and so far, countries have invested a lot of manpower and financial resources to improve the conductivity and cycle stability of lithium-sulfur battery. Zhang et al. prepared a three-dimensional porous graphene C_3N_4 composite material by microemulsion assembly, which was used as a cathode material for lithium-sulfur batteries [6]. Ji et al. reduces the dissolution of polysulfide by fixing sulfur and polysulfide on graphene oxide [7]. Lin et al. improves the efficiency of graphene sulfur composites through nitrogen doping [8]. Xu et al. synthesized S/3D graphene composite, and after recycling several times, the initial discharge capacity was 1260mAh/g, and a reversible capacity was 700mAh/g. The ion transport of the porous electrode structure provides a conductive path [9]. Zheng et al. optimized the hollow carbon nanofiber / sulfur composite by nitrogen doping and obtained a

reversible capacity of 625mAh/g and 513mAh/g after 100 cycles at current rates of 0.2 C and 0.5 C [10].

However, at present, lithium sulfur batteries still face issues such as poor cycling performance and actual energy density far lower than theoretical energy density, which restrict their practical application. Essentially, these issues are mainly related to the complex sulfur multi-step electrochemical reduction reaction (discharge) and Li_2S electrochemical oxidation reaction (charge) during battery charging and discharging. In order to improve and control the rate and conversion rate of these electrochemical and chemical reactions in the battery during charging and discharging, this article focuses on the influence of electrode thickness on the battery discharge process, Quantitative simulation analysis of battery discharge process under different electrode thickness parameters to obtain the influence of it on the apparent discharge performance of the battery.

The rest of the paper is arranged as follows. The model for the charging and discharging process of lithium-sulfur battery are presented in Section II. Analysis of the model and conclusion are developed in Section III and Section IV, respectively.

2. The Model for Charging and Discharging Process of Li-S Battery

The typical structure of the Li-S cells is shown in Figure 2. Lithium oxidation reaction mainly occurs on the lithium anode side during the discharge process, the electron is transmitted back to the sulfur positive electrode through the external circuit, the lithium ions diffuse and migrate to the sulfur positive electrode through the electrolyte, and chemically react with sulfur (dissolved S_8) at the interface. As the reduction reaction proceeds, different polysulfides (Li_2S_x) with different sulfur chain lengths are formed. Due to the differential solubility of the different polysulfides in the electrolyte, some polysulfide ions with high solubility such as (S_6^{2-}) will even migrate to the negative electrode and directly react with lithium. Polysulfides with low solubility (Li_2S_2, Li_2S) are gradually deposited at the reaction interface during the reaction process, reducing the reaction surface area and blocking the electrode pore channels until the discharge process cannot continue smoothly. In the process of lithium ion diffusion, migration back to the lithium negative side and with the external circuit conduction electron electrochemical reduction reaction form lithium, sulfur positive electrode polysulfide after gradually electrochemical oxidation reaction, eventually in the form of solid S8 deposited in the positive pore. Obviously, the sulfur positive electrode is the key to determine the performance of Li-S battery.

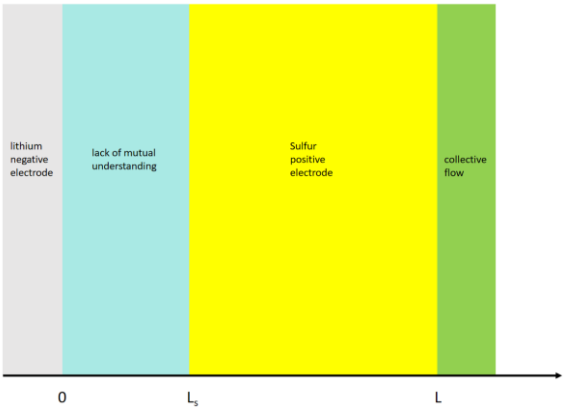

Figure 2: The model of lithium-sulfur battery.

2.1. The Model for Discharging Process of Li-S Battery

According to the model setting, the lithium anode is treated as the left boundary of the

diaphragm, and only the diaphragm and the sulfur positive electrode region are measured.

For the sulfur positive electrode region, the reaction components involved are Li^+, S_8, S_8^{2-}, S_6^{2-}, S_4^{2-}, S_2^{2-}, S^{2-}. For the above components i, considering the reaction, diffusion and migration in the positive electrode pore, the concentration of component i over time can be established as follows

$$\frac{\partial \alpha C_i}{\partial t} = -\nabla N_i + R_i - R_k, \tag{4}$$

where α is positive pole porosity, C_i is the molar concentration of i, R_i is electrochemical generation rate of component i and R_k is chemical generation rate of component i.

The flux N_i of component i is based on the dilute solution theory considering diffusion and electric field migration, which can be expanded as

$$\frac{N_i}{\alpha} = -D_i \nabla C_i - q_i \frac{D_i F C_i \nabla \phi}{RT}, \tag{5}$$

where D_i is the effective diffusion coefficient, q_i is the charge number of the component i, R is ideal gas constant, T is temperature, F is faraday constant and ϕ is fluid phase potential.

R_i is the sum of the reaction rate of component i in all the electrochemical reactions j in which component i participates, and R_i can be expanded as

$$R_i = \sum_j r_j = -a \sum_j \frac{s_{i,j} i_j}{n_j F}, \tag{6}$$

where a is the reaction ratio surface area, $s_{i,j}$ is the the anode reaction stoichiometric coefficient of a component i in the electrochemical reaction j, i_j is surface current density and n_j is reaction j transfers the electron numbers.

R_k is the sum of the reaction rate of component i in all the chemical reactions k in which component i participates, and R_k can be expanded as

$$R_k = \sum_k \beta_{i,k} r_k, \tag{7}$$

where $\beta_{i,k}$ is the molar number of ions i in precipitate k.

At the left boundary of the diaphragm $x = 0$, the electrochemical oxidation reaction of cathode lithium occurs at the interface according to the model. Therefore, at this boundary, the flux of the remaining ion component i is 0 except by the Li^+ flux of the electrochemical oxidation reaction of lithium metal, and the corresponding boundary conditions are:

$$N_i = 0, \qquad x = 0, \tag{8}$$

$$N_{L_i^+} = \frac{i_{L_i^+}}{F}, \qquad x = 0. \tag{9}$$

At the boundary $x = L_s$, set the flux $N_{i,l}$ of component i leaving the diaphragm, and the diaphragm is equal to the flux $N_{i,s}$ entering the sulfur positive electrode, so the boundary conditions are

$$N_{i,l} = N_{i,s}, \qquad x = L_s. \tag{10}$$

At the right boundary of the sulfur positive electrode $x = L$, all components i cannot pass through the collector fluid, so the flux of component i at the right boundary is 0, and the boundary condition is

$$N_i = 0, \qquad x = L. \tag{11}$$

2.2. The Model for Charging Process of Li-S Battery

For the Li-S battery charging process, the oxidation reactant in the starting sulfur positive electrode of charging is Li_2S, and the volume fraction of Li_2S increases with the beginning of charging. The change pattern of α_{k,Li_2S} over time t can be described as

$$\frac{\partial \alpha_{k,Li_2S}}{\partial t} = V_{k,Li_2S}(r_{j,Li_2S} + r_m), \tag{12}$$

where V_{k,Li_2S} is the molar volume of the solid-phase Li_2S, r_{j,Li_2S} represents the Li_2S depletion resulting from the electrochemical reactions involving Li_2S, r_m is the chemical rate of the redox-mediated reaction.

For the charging components Li^+, $S_8^{2-}$and S_4^{2-}, the balance equation can be expanded as:

$$\frac{\partial \alpha C_i}{\partial t} = -\nabla N_i + R_i + r_m. \tag{13}$$

The transmission process of the components in the diaphragm should be appropriately simplified. Only the transmission of lithium ions is considered in the diaphragm, and the transmission of other components in the diaphragm is not considered anymore.

$$\frac{\partial \alpha C_i}{\partial t} = -\nabla N_i + R_i. \tag{14}$$

The boundary conditions required for solving the above balance equation are given below:

At the left boundary of the diaphragm $x = 0$, the electrochemical reduction reaction of the negative electrode lithium occurs at the interface, corresponding to the boundary conditions of:

$$N_{L_i^+} = \frac{i_{L_i^+}}{F}, \qquad x = 0. \tag{15}$$

At the junction of the diaphragm and the sulfur positive electrode $x = L_s$, the flux $N_{i,l}$ from the diaphragm is set, and the flux $N_{i,s}$ into the sulfur positive electrode are equal. The boundary conditions are

$$N_{i,l} = N_{i,s}, \qquad x = L_s. \tag{16}$$

Since only lithium ion transport is considered in the diaphragm, the flux of other components is 0 at $x = L_s$, namely:

$$N_i = 0, \qquad x = L_s. \tag{17}$$

At the $x = L$ at the right boundary, the flux of component i at the right boundary is 0, and the

boundary conditions are also:

$$N_i = 0, \qquad x = L. \tag{18}$$

3. Analysis of the Model

3.1 Model Parameter

Table 1: Concentration of the ionic components of the Li-S battery.

component i	Li^+	S_8	S_8^{2-}	S_6^{2-}	S_4^{2-}	S_2^{2-}	S^{2-}
$C_i\ (mol/m^3)$	1000	20	0.2	0.3	0.02	5×10^{-7}	8×10^{-10}

3.2 Result Analysis and Discussion

The amount of sulfur load on the sulfur positive electrode of a lithium sulfur battery is an important factor determining the actual capacity of the battery, and the amount of sulfur load on a unit area electrode is determined by the electrode thickness. Obviously, under a certain proportion of sulfur material in the electrode, the sulfur load of the active material on the positive electrode per unit area will increase proportionally with the increase of electrode thickness. However, as the electrode thickness increases, it is affected by factors such as transmission and reaction, the conversion and utilization rate of sulfur in the electrode cannot be consistent with that when the electrode thickness is low. Therefore, this article simulates and analyzes the effect of changing the cathode thickness on the discharge process of lithium sulfur batteries under a certain sulfur volume fraction in the cathode. The reference concentrations of each ion component involved in the electrochemical reaction in the model are shown in Table 1.

According to the B-V equation, the exchange current density i_0 is the core parameter describing the intrinsic electrochemical reaction rate, and the change of i_0 affects the size of the corresponding electrochemical reaction rate. Therefore, this section calculates the effect of the exchange current density i_0 in the change of $L_i \rightarrow L_i^+$ electrochemical oxidation reaction and $S_8 \rightarrow S_8^{2-} \rightarrow S_6^{2-} \rightarrow S_4^{2-} \rightarrow S_2^{2-} \rightarrow S^{2-}$ multi-step electrochemical reduction reaction on the discharge performance of lithium-sulfur batteries with different positive thicknesses when other conditions remain unchanged.

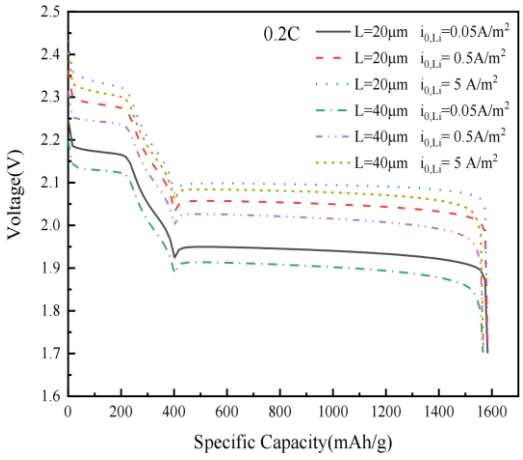

Figure 3: The Effect of $i_{0,Li}$ on battery discharge under different positive electrode thicknesses.

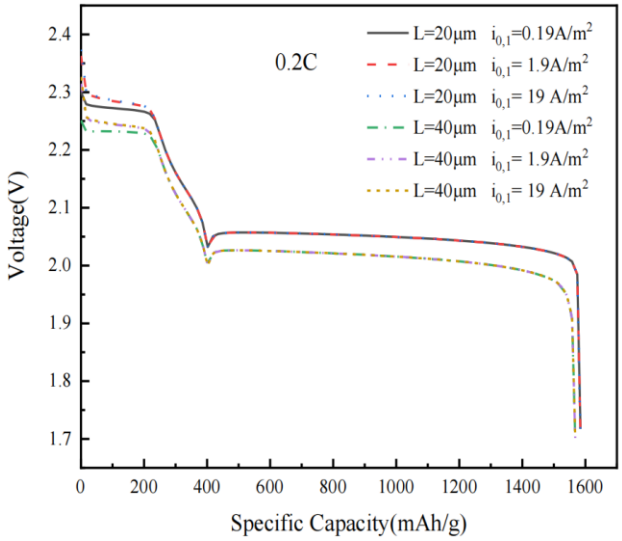

Figure 4: The Effect of $i_{0,1}$ on battery discharge under different positive electrode thicknesses.

Figure 3 shows the constant current discharge curves of the negative electrode $L_i \rightarrow L_i^+$ electrochemical oxidation reaction under a discharge rate of 0.2 C, with exchange current densities $i_{0,Li}$ of 0.05, 0.5, and 5 A/m^2, and positive electrode thicknesses of 20μm and 40μm, respectively; From the Figure 3, it can be seen that the discharge curve presents a typical two platform discharge characteristic of lithium sulfur batteries. At the same electrode thickness, the discharge curve shifts upwards as $i_{0,Li}$ increases, indicating that as the rate of lithium electrochemical oxidation reaction on the negative electrode increases, the overpotential required to maintain the same discharge current density decreases; Comparing the constant current discharge curves of three different exchange current densities $i_{0,Li}$ under different thicknesses, it can be seen that under the same $i_{0,Li}$, the discharge potential of the 40μm thick positive electrode is lower, indicating that at the same lithium electrochemical reaction rate, due to the increase in positive electrode thickness, maintaining the same rate of discharge requires a higher overpotential; Moreover, it can be seen from the graph that the discharge specific capacity of the 40μm thick positive electrode is slightly lower than that of the 20μm thick positive electrode, indicating that as the thickness of the positive electrode increases, the utilization rate of sulfur in the positive electrode will decrease.

For the reaction process $S_8 \rightarrow S_8^{2-} \rightarrow S_6^{2-} \rightarrow S_4^{2-} \rightarrow S_2^{2-} \rightarrow S^{2-}$ that occurs on the positive electrode, the exchange current density of these five conversion processes is recorded as $i_{0,1}(S_8 \rightarrow S_8^{2-})$, $i_{0,2}(S_8^{2-} \rightarrow S_6^{2-})$, $i_{0,3}(S_6^{2-} \rightarrow S_4^{2-})$, $i_{0,4}(S_4^{2-} \rightarrow S_2^{2-})$ and $i_{0,5}(S_2^{2-} \rightarrow S^{2-})$.

Figure 4 shows the exchange current densities $i_{0,1}$ of the dissolved $S_8 \rightarrow S_8^{2-}$ electrochemical reduction reaction in the positive electrode of the battery at a rate of 0.2 C discharge, with values of 0.19, 1.9, and 19 A/m^2, respectively, and positive electrode thicknesses of 20 and 40μm Constant current discharge curve under m; From the graph, it can be seen that the difference in constant current discharge curves under different i0s is mainly reflected in the first discharge platform. As $i_{0,1}$ increases, the potential of the first discharge platform increases, indicating that this platform discharge is mainly related to the reduction reaction of $S_8 \rightarrow S_8^{2-}$. The faster the electrochemical reduction reaction rate, the smaller the reaction overpotential, and the higher the discharge platform potential; At the same time, it can be observed that when the exchange current densities $i_{0,1}$ are 1.9

A/m^2 and 19 A/m^2, the constant current discharge curves are close to overlapping, indicating that the electrochemical reduction reaction is already under transfer control when the exchange current density $i_{0,1}$ is 1.9 A/m^2 under 0.2 C rate discharge, and the dissolution rate of sulfur in the electrolyte is more affected at this time; The comparison of constant current discharge curves under two different positive electrode thicknesses shows that except for the difference in the first discharge platform, all other differences are not closely related to the rate of $S_8 \rightarrow S_8^{2-}$ electrochemical reduction reaction.

Figures 5 and 6 show the constant current discharge curves of two electrochemical reduction reactions of $S_8^{2-} \rightarrow S_6^{2-}$ and $S_6^{2-} \rightarrow S_4^{2-}$ under different exchange current densities $i_{0,2}$, $i_{0,3}$, and different cathode thicknesses, respectively. These two reactions begin to occur at the first discharge platform, but mainly occur in the transition section between the first discharge platform and the second discharge platform. From the calculation results, as the $i_{0,2}$ of the $S_8^{2-} \rightarrow S_6^{2-}$ reaction changes in Figure 5, there is no significant difference in the constant current discharge curve, indicating that the change in the electrochemical reduction reaction rate does not have a significant impact on the discharge process. It can also be considered that in the multi-step sulfur reduction process. This reaction will not be a control step of the process. As the $i_{0,3}$ of the $S_6^{2-} \rightarrow S_4^{2-}$ reaction changes in Figure 6, there is a slight change in the constant current discharge curve in the transition section from the first discharge platform to the second discharge platform. From the figure, it can be seen that when $i_{0,3}$ increases from 2×10^{-5} A/m^2 to 2×10^{-2} A/m^2, the discharge potential in the transition section increases by about 10mV, and when it continues to increase to 2 A/m^2, the discharge potential remains basically unchanged, indicating that the electrochemical reduction reaction of $S_6^{2-} \rightarrow S_4^{2-}$ will not be a controlling step in the sulfur reduction process.

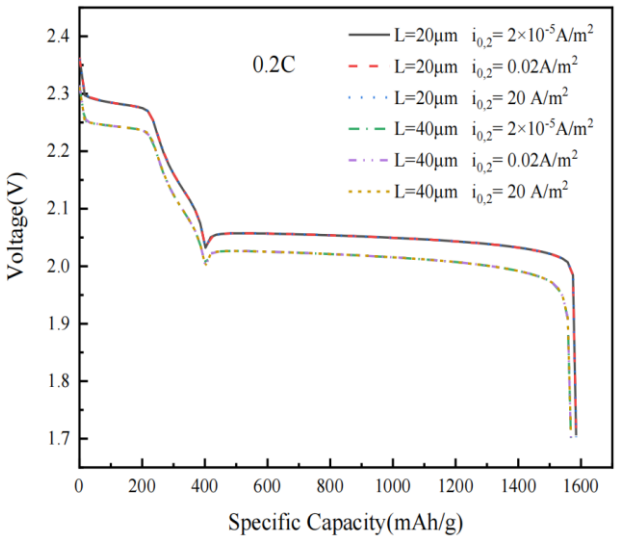

Figure 5: The Effect of $i_{0,2}$ on battery discharge under different positive electrode thicknesses.

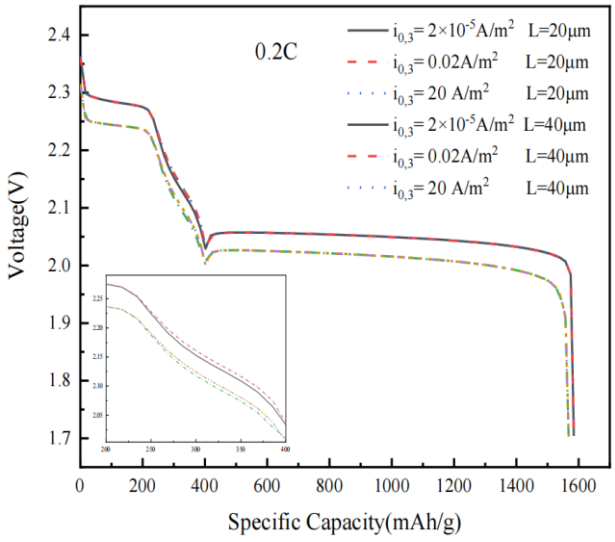

Figure 6: The Effect of $i_{0,3}$ on battery discharge under different positive electrode thicknesses.

Figure 7 shows the exchange current densities $i_{0,4}$ of the electrochemical reduction reaction of $S_4^{2-} \rightarrow S_2^{2-}$ in the positive electrode of the battery at a rate of 0.2 C discharge, which are 2×10^{-6}, 2×10^{-4}, and 2×10^{-2} A/m^2, respectively, with positive electrode thicknesses of constant current discharge curve under 20 and 40μm; From the graph, it can be seen that the change in the electrochemical reduction reaction rate mainly changes the potential of the second discharge platform region. Compared to 20μm, the potential of the second discharge platform region of the positive electrode with a thickness of m at an exchange current density of 2×10^{-6} and 2×10^{-4} A/m^2 is about 20mV when the discharge specific capacity is 400mAh/g. The potential difference gradually increases as the discharge process progresses. When the discharge specific capacity reaches 1550mAh/g, the potential difference reaches about 100mV, indicating that as the reduction reaction proceeds, the concentration of S_4^{2-} ions decreases, The reaction kinetics have gradually become the controlling factor of the reaction process, and in order to maintain the discharge current density, higher and higher overpotentials are required; When the exchange current density increases from 2×10^{-4} A/m^2 to 2×10^{-2} A/m^2, the change in discharge potential is not significant, which should be related to the influence of the conversion rate of $S_2^{2-} \rightarrow S^{2-}$ on the subsequent reaction; When the electrode thickness increases to 40μm, it still shows the same trend of change, especially when the discharge is close to the cut-off point. Due to the increase in electrode thickness, the ion transfer effect is greater. Similarly, when the discharge specific capacity reaches 1550mAh/g, the potential difference is much greater than 100mV.

Figure 8 shows the exchange current densities $i_{0,5}$ of the electrochemical reduction reaction of $S_2^{2-} \rightarrow S^{2-}$ in the positive electrode of the battery at a rate of 0.2 C discharge, which are 2×10^{-8}, 2×10^{-7}, and 2×10^{-6} A/m^2, respectively, with positive electrode thicknesses of constant current discharge curve under 20 and 40μm; Similar to the trend after the change in electrochemical reduction reaction rate of $S_4^{2-} \rightarrow S_2^{2-}$, the change in electrochemical reduction reaction rate of $S_2^{2-} \rightarrow S^{2-}$ mainly causes a change in the potential of the second discharge platform, as can be clearly seen from the graph 20μm positive electrode, when the exchange current density $i_{0,5}$ is

2×10^{-8} A/m^2, the platform potential is around 2.0V. When $i_{0,5}$ increases to 2×10^{-7} A/m^2, the platform potential exceeds 2.05V. Continuing to increase $i_{0,5}$ to 2×10^{-6} A/m^2, the platform potential is around 2.1V. This indicates that the impact of the $S_2^{2-} \rightarrow S^{2-}$ electrochemical reduction reaction on the second platform stage is greater than that of the $S_4^{2-} \rightarrow S_2^{2-}$ electrochemical reduction reaction. At higher values of $i_{0,5}$, there is a change in the starting region of the second platform where the potential decreases and then rebounds. This is clearly due to the increase in S_2^{2-} concentration, which accelerates the reaction rate and reduces the overpotential of the $S_2^{2-} \rightarrow S^{2-}$ reaction, resulting in an increase in the corresponding discharge potential. When the electrode thickness increases to 40μm, except for a decrease in specific capacity, the main change is that the overall potential of the second discharge platform has decreased, with a decrease range of about 20 to 40mV.

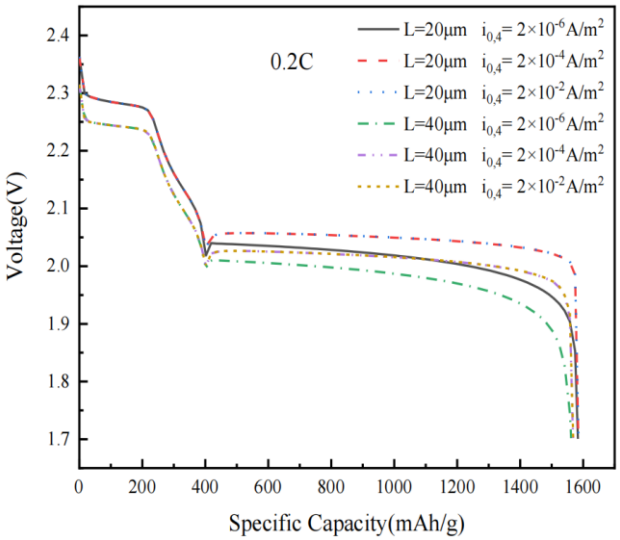

Figure 7: The Effect of $i_{0,4}$ on battery discharge under different positive electrode thicknesses.

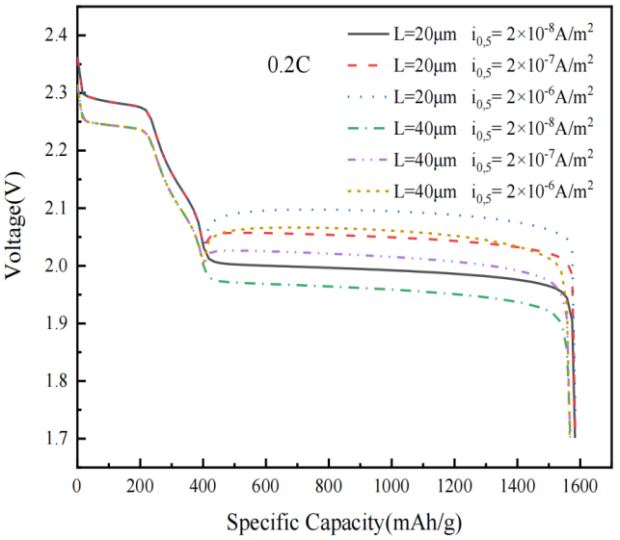

Figure 8: The Effect of $i_{0,5}$ on battery discharge under different positive electrode thicknesses.

4. Conclusions

This article investigates the effect of different sulfur cathode thicknesses on the performance of lithium-sulfur batteries. Simulation results of the oxidation reaction of the lithium negative electrode and the multi-step reduction reaction of the sulfur positive electrode under different reaction rate constants show that the increase of oxidation reaction rate of the negative electrode is conducive to improving the battery discharge performance. In the multi-step reduction reaction, appropriately increasing the reaction rate of $S_8 \rightarrow S_8^{2-}$ is beneficial to improve the discharge potential of the first discharge platform. The reaction rates of $S_8^{2-} \rightarrow S_6^{2-}$ and $S_6^{2-} \rightarrow S_4^{2-}$ will not be a control step in the multistep reduction reaction process. The reaction rates of $S_4^{2-} \rightarrow S_2^{2-}$ and $S_2^{2-} \rightarrow S^{2-}$ have a great impact on the second discharge platform, especially the $S_2^{2-} \rightarrow S^{2-}$ reaction, increasing its reaction rate is very important to improve the battery discharge performance. The comparative results of changing the electrochemical reaction rate and changing the electrode thickness show that when the thickness increases, the discharge specific capacity will decrease slightly, and the reaction overpotential will increase.

References

[1] Chou, S., Pan, Y., Wang, J., Liu, H., Dou, S., Three-dimensional growth of Li_2S in lithium-sulfur batteries promoted by a redox mediator[J]. Nano Letters. 16 (2014) 20347–20359.

[2] D€orfler, S., Althues, H., H€artel, P., Abendroth, T., Schumm, B., Kaskel, S., Carbon@titanium nitride dual shell nanospheres as multi-functional hosts for lithium sulfur batteries[J]. Energy Storage Materials. 4 (2020) 539–554.

[3] Balach, J., Jaumann, T., Klose, M., Oswald, S., Eckert, S., Giebeler, L., Cobalt-doped vanadium nitride yolk shell nanospheres@carbon with physical and chemical synergistic effects for advanced Li-S Batteries [J]. ACS Applied Materials & Interfaces. 25 (2015) 5285–5291.

[4] Betz, J., Bieker, G., Meister, P., Placke, T., Winter, M., Schmuch, R., Rational design of porous nitrogen-doped Ti3C2 MXene as a multifunctional electrocatalyst for Li-S chemistry[J]. Nano Energy. 9 (2019) 1803170.

[5] Levin, B., Zachman, M., Werner, J., Sahore, R., Nguyen, K., Han, Y., Xie, B., Ma, L., Archer, L., Giannelis, E., Wiesner, U., Kourkoutis, L., Muller, D., Electrocatalysis of polysulfide conversion by sulfur-deficient MoS2 nanoflakes for lithium-sulfur batteries[J]. Energy & Environmental Science. 23 (2017) 155–162.

[6] Zhang, J.,Li, J.,Wang, W., Microemulsion assisted assembly of 3D porous S /graphene@ g-C3N4 hybrid sponge as free-standing cathodes for high energy density Li-S batteries[J]. Advanced Energy Materials, 2018, 8(14) : 1702839.

[7] Yue, Z., Cairns, E., Li, J., Graphene Oxide as a Sulfur Immobilizer in High Performance Lithium/Sulfur Cells [J]. Journal of the American Chemical Society, 2011, 133(46): 18522-18525.

[8] Lin, T., Tang, Y., Wang, Y., Scotch-tape-like exfoliation of graphite assisted with elemental sulfur and graphene–sulfur composites for high-performance lithium-sulfur batteries [J]. Energy & Environmental Science, 2013, 6(4): 1283-1290.

[9] Xu, C., Wu, Y., Zhao, X., Sulfur/three-dimensional graphene composite for high performance lithium–sulfur batteries [J]. Journal of Power Sources, 2015, 275: 22-25.

[10] Zheng, G., Yang, Y., Cha, J. Hollow carbon nanofiber-encapsulated sulfur cathodes for high specific capacity rechargeable lithium batteries [J]. Nano letters, 2011, 11(10): 4462-4467.